Time-sequential Sampling and Reconstruction of Tone and Color Reproduction Functions for Xerographic Printing

Perry Y. Li, Teck-Ping Sim and Dongjun Lee

Abstract— **Tone and color reproduction functions (TRC or CRC) characterize how a printer maps a desired tone or color into the actual output. Ideally, the TRC/CRC should be identity maps. Sensing the TRC/CRC is needed for closed loop feedback control. Currently, sensing of the high dimensional TRC/CRC is limited since only a small number of tone/color sensor patches can be printed and measured at a time. Time-sequential sampling is proposed to alleviate this difficulty by sampling different tones/colors at different times. A Kalman filtering approach is proposed to reconstruct the TRC/CRC from the time-sequential samples. The effect of two sampling strategies - lexicographical and bit-reversed strategies are analyzed. It is shown that the periodic Kalman reconstruction filter is effective, and that it can be interpreted to consist of cascade of modulation, low pass and demodulation processes.**

I. Introduction

A color xerographic (i.e. laser) printer can be considered a mapping between the desired image and the output image. An important performance criterion for a color printer is that any desired colors in the desired customer image is faithfully reproduced. By ignoring the spatial dimension (such as lines and textures) of print quality for the moment and focusing on the issue of consistent color reproduction only, a color xerographic printer can be represented by the color reproduction function: CRC : $\mathcal{C} \to \mathcal{C}$, desired color $\mapsto$ output-color, where $\mathcal{C}$ is a 3-dimensional color space. An ideal printer is the one in which the CRC is an identity function.

A digital color xerographic printer generates color by printing and overlaying the Cyan, Magenta, Yellow and blacK (CYMK) separations. The printing of each color separation is characterized by the tone reproduction curve (TRC):TRC : $[0, 1] \to \mathcal{C}$, desired tone $\mapsto$ output-color, where the tone τ of the separation is the solidness of the primary toner color. For example, a patch with $\tau = 0.1$ for the magenta color separation corresponds to a light violet whereas $\tau = 1.0$ corresponds to solid magenta color. Physically, the tone of the primary separations are determined by the pattern and size of the half tone dots printed. Roughly speaking, the denser and bigger the dots are, the more solid the color. The final color printed is a composition of the colors of the individual separation. Thus, the so called Image Output Terminal (IOT) portion of the printer can be considered a mapping IOT : $(t_C, t_Y, t_M, t_K) \mapsto$ output-color where (t_C, t_Y, t_M, t_K) are the tones for the four color separations.

The xerographic printing process is subject to disturbances from many factors including temperature, humidity, material age and variations etc.. Several xerographic actuators such as laser power, corotron voltage and development / bias voltages can be used to combat these variations. The goal of the xerographic color control system is to ensure that the CRC is as close to the identity map as possible. Unlike the control objective for most processes which is to control or regulate the output of the process, the color control problem consists in maintaining the *process itself* to be constant and stable. The difference is due to the fact that every customer image to be printed can contain *many* and *any* possible colors which the xerographic printer must reproduce correctly all at once. Moreover, xerographic printers are often used in an on-demand manner in which consecutive customer images are different.

A similar, but simpler control problem can be formulated for the printing of each color separation. In this case, the control objective is to maintain and stabilize the tone reproduction curve (TRC) for each separation [1]. If the manner in which the primary colors are combined is stable and constant, then output color will also consistent when the TRC for each separation has been effectively stabilized.

Both the CRC and TRC control formulations pose significant problems for sensing and control. It is because both the CRC and TRC as mappings are potentially infinite dimensional whereas there are only a small number actuators and sensors available. Even when each color coordinate is modestly discretized into 16 steps, the color quality of $16^3 = 100K$ desired colors need to be kept track of for the color control problem, and 16 tones must be kept track of for the TRC control problem for each separation. A solution to this control problem has been addressed previously for the TRC stabilization problem in [1] using a curve-fitting technique. The sensing issue is addressed in the present paper.

Feedback control for the stabilization of the TRC or CRC such as in [1] requires sensing of the TRC or the CRC. Process sensing for the xerographic printing process consists in printing small color patches in the unused areas of the photoreceptor and measuring the density or color of the patches. Typically, only 3 to 5 patches are to be printed every few photoreceptor belt cycles. This amounts to sampling either the TRC or the CRC at 3 to 5 points once in a while. Compared to the potentially large dimensionality of the TRC or CRC to be controlled, this limited sensing

Research supported by the National Science Foundation CMS-0201622
Please send all correspondence to Perry Y. Li. The authors are with the Department of Mechanical Engineering, University of Minnesota, 111 Church St. SE, Minneapolis MN 55455. E-mails: {pli,tpsim,djlee}@me.umn.edu.

capability poses a significant difficulty for feedback control.

In this paper, time-sequential sampling strategy is proposed to increase the utility of the available feedback information. Time-sequential sampling was investigated in the 1980's and 1990's for video and time varying imaging applications (e.g. video and tomography) [2], [3], [4], [5], [6], [7]. For time varying images, time-sequential sampling refers to sampling the image at different spatial locations at different sampling instances. Rastering in television is an illustration. The benefit is that by trading off temporal bandwidth with spatial bandwidth, the temporal bandwidth of the time varying image that can be captured faithfully beyond the Nyquist rate determined by the periodicity of the sampling scheme alone. In another perspective, the sampling rate can be reduced while retaining the same information content. In our context, time-sequential sampling means that at different sampling instances, different tones or different colors are sampled. This maximizes the information from the TRC/CRC samples and allows the time varying CRC or TRC to be captured (and subsequently reconstructed faithfully) even when only a small number of samples of the CRC / TRC are available at each instant.

The rest of the paper is organized as follows. In section II, the time sequential sampling approach for tone reproduction curves is formulated. Section III presents the spectral content of time-sequentially sampled signals. Section IV presents a Kalman filter approach to TRC reconstruction from time-sequential samples. Section V presents an interpretation of the periodic Kalman reconstruction filter. Section VI contains some concluding remarks.

II. Time sequential sampling

Consider the time varying TRC$(k) \in \{\mathcal{F} : [0,1] \to \mathcal{C}\}$ where $k = 0, 1, \ldots$ denotes the time indices. The time variation is due to disturbances or control actuation. Suppose at each sampling instant k, n tones given by $[\alpha_1(k), \alpha_2(k), \ldots \alpha_n(k)]$ are printed and measured. We call $\alpha : \mathcal{Z} \to [0,1]^n$, $k \mapsto [\alpha_1(k), \alpha_2(k), \ldots, \alpha_n(k)]$ the sampling sequence. The time sequentially sampled TRC_s is given by: for $k = 0, 1, \ldots$,

$$TRC_s(k) = TRC(k)[\alpha(k)] = \begin{pmatrix} TRC(k)[\alpha_1(k)] \\ TRC(k)[\alpha_2(k)] \\ \vdots \\ TRC(k)[\alpha_n(k)] \end{pmatrix}$$

In our research, we restrict α to be $M-$periodic, i.e. $\alpha(k+M) = \alpha(k)$ for all $k \in \mathcal{Z}$, and $n = 1$.

We consider the following questions:

1. Given $TRC_s(k)$, the time sequentially sampled TRC for $k = 0, 1, \ldots, KT$, obtained using a periodic time-sequential sampling sequence $\alpha(\cdot)$,how does one reconstruct $TRC(KT)$. We are particularly interested in causal reconstruction so that the reconstruction at time t only requires measurements at $kT \leq t$.
2. How do sampling sequences affect the reconstruction accuracies? Suppose that we have determined that there are M tones $\tau_0, \ldots, \tau_{M-1}$ that will be sampled. Let $g : k \mapsto \tau_k$ be a monotone map that maps the index to the actual tone. We focus particularly on two sampling sequences:

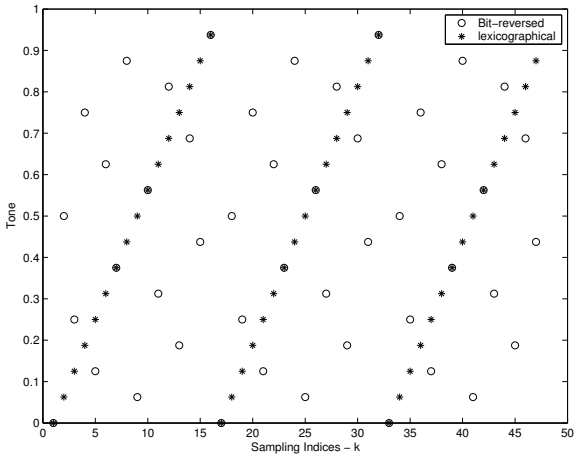

Fig. 1. Bit Reversed and Lexicographical Time-sequential sampling sequence with $M = 16$ points.

- **Lexicographic**: *Here* $\alpha(k) = g(\alpha_g(k))$ *and* $\alpha_g(k) := mod(k, M))$ *so that the order of sampling is according to its index.*
- **Bit reversed**: *Here* $\alpha_g(k)$ *is given by 1) representing the index* k *as a binary number, 2) reversing the order of the significant bits. Finally,* $\alpha(k) = g(\alpha_g(k))$. *The idea of the bit-reversed order is that it is roughly an even sampling of the time-tone space.*

These two sequences ($\alpha_g(k)$) are shown in Fig. 1. It is apparent that the lexicographical sequence does not cover the spatial-temporal domains as evenly as the bit-reversed sequence. In the rest of the paper, we interchange the use between $\alpha(k)$ and the corresponding tone index $\alpha_g(k)$.

Exactly the same approach can be applied to a color reproduction curve. In this case the sampling sequence is: $\alpha : \mathcal{Z} \to \mathcal{C}^n$ since CRC is to be sampled at n colors. The benefits of time-sequential sampling is will be even more important since the dimensionality of the CRC is larger.

III. Spectral Content of Time-sequentially sampled TRC

Let $\omega(\tau, t) \in \Re$ be a tonal-temporal signal such as a TRC. Allebach [2] shows that the fourier transform of a time-sequentially sampled signal is given by the original spectrum $\Omega(u, f)$ (u is the tonal frequency, f is the temporal frequency), aliased by its weighted tonal and temporal frequency translates:

$$\Omega_s(u, f) = \sum_{m,p} Q_{mp} \Omega(u - m/A, f - p/B)$$

$$Q_{mp} = \frac{1}{M} \sum_{l=0}^{M-1} exp^{-j\frac{2\pi}{M}(m\alpha(l)+pl)}$$

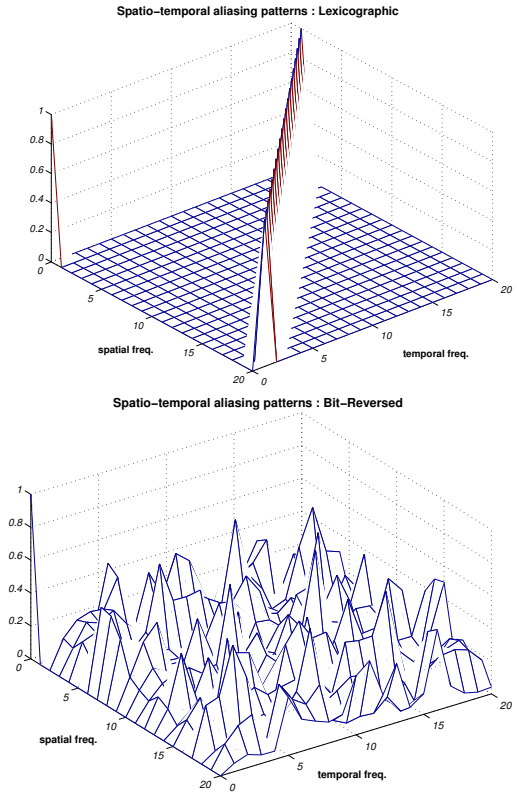

Fig. 2. Aliasing weights Q_{mp} for lexicographical (top) and bit-reversed sequences (bottom). The tonal (spatial)

where $B = MT$ is the periodicity of the sampling sequence and A/M is the tonal resolution with A being the tone range ($A = 1$ in our case). Notice that the frequency translates are given by $(m/A, p/B)$) when $Q_{mp} \neq 0$. Also, both the frequency translates and the weights depend on the sampling sequence.

If the TRC has a tonal frequency support less than $M/(2A)$, and a temporal frequency support less than $1/(2B) = 1/(2MT)$, then no-aliasing occurs. The original signal can (theoretically) be reconstructed perfectly via a low pass spatial/temporal filter. $M/(2A)$ and $1/(2B)$ are therefore the tonal and temporal Nyquist frequencies. Note that when M is large to satisfy its tonal (color) frequency requirements, $1/(2B)$ can be very small for time-sequentially sampled signal.

When the signal is temporally undersampled, the efficacies of different sampling sequences are related to the aliasing patterns.

For the lexicographic sequence and the bit-reversed sequence with $M = 21$, the aliasing patterns (Q_{mp}) for the lexicographical sequence and the bit-reversed sequence are shown in Fig. 2. The aliasing weights for the lexicographical sequence are concentrated on a line, whereas for the bit-reversed case, the weights are more evenly distributed, eventhough the sums of Q_{mp} for both sequences are the same. The consequence of this result is that for signals with low spatial / temporal bandwidths (e.g. if the signal support lies within the triangle, $\{(u, f)|u \leq M/2(1 - f \cdot 2T))\}$), the lexicographical sampling strategy has the potential of perfect reconstruction. On the other hand, although the bit-reversed sampling sequence cannot provide for perfect reconstruction, it is more tolerant to high temporal/spatial bandwidth signal.

IV. Reconstruction via a Kalman Filter

Assuming that no aliasing occurs, traditionally, time-sequentially sampled signals are reconstructed by low pass temporal-spatial filtering based on the assumed signal spectral support. This approach, however, is problematic in feedback control application for the following reasons:

- The ideal low pass filter cannot be implemented causally.
- When the reconstructed TRC is used for feedback control, the frequency content of the TRC will be significantly increased due to the control input. This induce undue aliasing, while the inherent process dynamics actually remains the same. However, it is not apparent how to incorporate the known information about the control input in the low-pass reconstruction technique.

These difficulties can be resolved using an alternate approach based on Kalman filtering.

We assume that the TRC is well represented by its values at $M = 21$ tones so that $TRC(k) \in \Re^{M=21}$. To exhibit its tonal spectral contents, we further parameterize $TRC(k)$ by its DFT so that:

$$TRC(k) = G \cdot x(k)$$

where $k \in \mathcal{Z}^+$ is the time index, $G \in \Re^{M \times M}$ is a matrix of Fourier basis functions and $x(k) \in \Re^M$ is the vector of Fourier coefficients.

For simplicity, we model the TRC dynamics as having random drifts $w(k)$, and the time-sequentially sampled signal is subject to measurement noise $n(k)$:

$$\begin{aligned} x(k+1) &= x(k) + w(k) \\ TRC_s(k) &= C_\alpha(k) G \cdot x(k) + n(k) \end{aligned} \tag{1}$$

where $C_\alpha(k) \in \Re^{1 \times M}$ is a M-periodic sampling matrix for the time-sequential sampling pattern $\alpha(k)$. It has a 1 at the $\alpha(k)$ index (actually the $\alpha_g(k)$-th entry), and 0 at other locations. In our study, we assume that $w(k)$ and $n(k)$ are zero mean white noise sequences with covariances R_{ww} and R_{nn}. However, the model can be easily generalized when they are pink noise sequences. This will be useful for making tonal-temporal frequency tradeoffs. Effect of control actuators can also be easily incorporated into (1). For simplicity, we assume that in (1), the effect of controls have been subtracted out.

In our study below, we use $M = 21$, $T = 0.4s$, $A = 1$, $1/B = 0.12Hz$ so that the tonal-temporal Nyquist frequencies are $(u, f) = (10.5\text{cycles/tone}, 0.06\text{Hz})$.

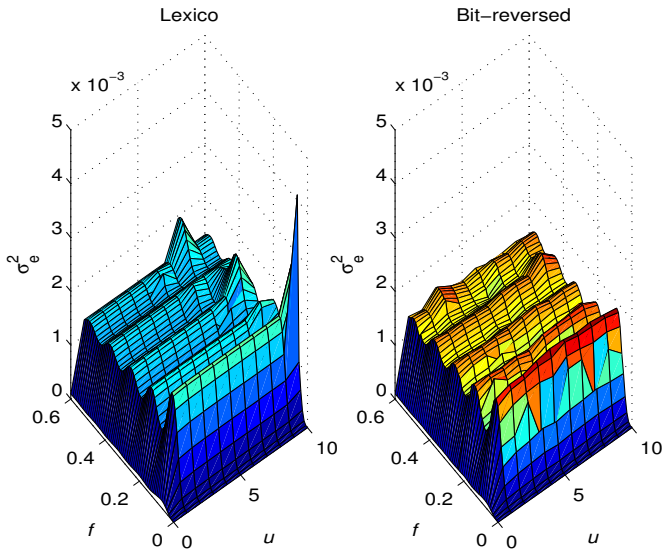

Fig. 3. Mean squared reconstruction errors σ_e^2 using lexicographical and bit-reversed sequences at various tonal-temporal frequencies (u, f).

Because span$\{C_\alpha(k), k = 0, \ldots, M-1\} = \Re^M$, Eq.(1) is a $M-$periodic observable linear system and admits a M-periodic Kalman filter in the steady state:

$$\begin{aligned} \hat{x}(k+1) &= A_c(k)\hat{x}(k+1) + B_c(k) \cdot TRC(k) \\ \widehat{TRC}(k) &= G\hat{x}(k+1) \end{aligned} \tag{2}$$

where

$$\begin{aligned} A_c(k) &= I - L(k)C_\alpha(k) \\ B_c(k) &= L(k)C_\alpha(k) \end{aligned}$$

and $L(k)$ is the periodic Kalman filter gain obtained by solving the periodic Riccati equation:

$$\begin{aligned} \bar{P}(k+1) &= \bar{P}(k) - L(k)C_\alpha(k)G\bar{P}(k) + R_{ww} \\ L(k) &= \bar{P}(k)G^T C_\alpha^T(k)\left[R_{nn} + C_\alpha(k)G\bar{P}(k)G^T C_\alpha^T(k)\right]^{-1} \\ \bar{P}(k) &= \bar{P}(k+M) \end{aligned} \tag{3}$$

In (2), the unsampled $TRC(k) \in \Re^M$ (instead of the time sequentially sampled $TRC_s(k) \in \Re$) is considered as the input to the Kalman filter and the reconstructed TRC, $\widehat{TRC}(k) \in \Re^M$ as the output.

To test the Kalman filter we generate the $TRC(k)$ by superimposing on a typical TRC a signal of the form $a \cdot cos(2\pi(u\tau - f \cdot t))$ which has a single tonal-temporal frequency (u, f). The mean squared reconstruction error,

$$\begin{aligned} \sigma_e^2 &:= \|TRC(\cdot) - \widehat{TRC}(\cdot)\|_2^2 \\ &:= \sum_k \|TRC(k) - \widehat{TRC}(k)\|_2^2 \end{aligned}$$

for each pair of (u, f) can be used to compare the filter performances at different frequencies. Fig. 3 shows the mean squared reconstruction errors of the Kalman filters using lexicographical, and bit-reversed sampling sequences.

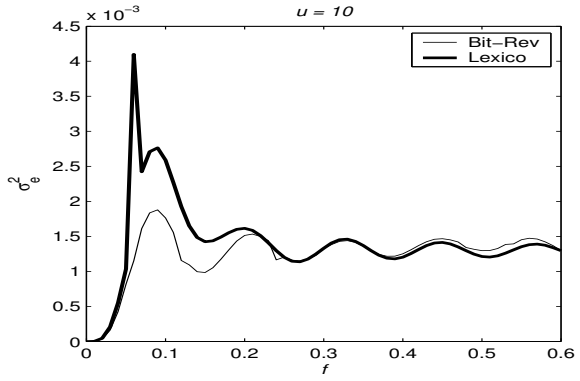

Fig. 4. σ_e^2 - mean squared reconstruction error at high spatial frequency and at various temporal frequencies.

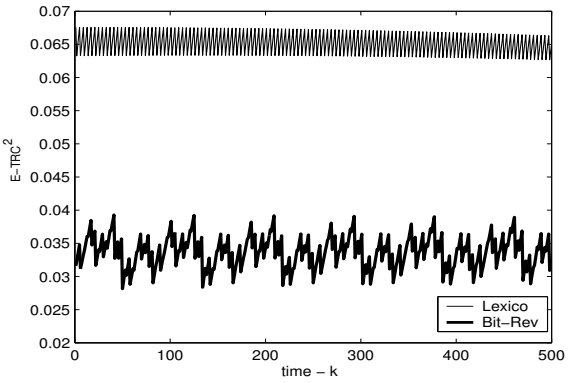

Fig. 5. Reconstruction error ($\|TRC(k) - \widehat{TRC}(k)\|_2^2$) as a function of time using lexicographical and bit-reversed sequences at $(u, f) = (10, 0.06)$

Notice that at low tonal-temporal frequencies, both filters reconstruct well. Noticeably, at high tonal frequencies (near the Nyguist frequency of $u = 10$), the Kalman filter for the lexicographical sequence reconstructs worse than the one for the bit-reversed sequence, especially near the temporal Nyguist frequency $f = 0.06Hz$. This result can also be seen from the actual reconstruction error in Fig. 4 and 5.

The mean-squared error does not convey the worst case error however. The worst case error (after convergence) for the two sampling strategies are shown in Figs. 6-7. They show that although perfect reconstruction is achieved at low temporal frequencies, the performance degrades as the tonal and temporal (u, f) frequencies increase. It also shows that with lexicographical strategy, the reconstructed TRC tends to be out-of-phase from the actual TRC. This causes the worst case error using the lexicographical strategy to be worse than that of the bit-reversed strategy. In both cases, the reconstruction at low tonal frequency ($u = 1$) and high temporal frequencies introduce high tonal frequency artifacts. This is present because the TRC signal model in Eq. (1) assumes that the TRC's spectral support is rectangular. If we had assumed that the tonal frequency content decreases as the temporal frequency content increases, then

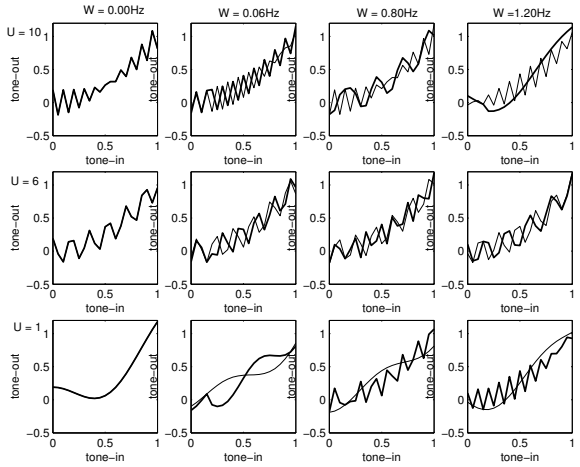

Fig. 6. Input TRC (consisting of a typical TRC with various single tonal-temporal frequency imposed on it) and its worst case steady state reconstruction, for Kalman filter designed for the lexicographic strategy.

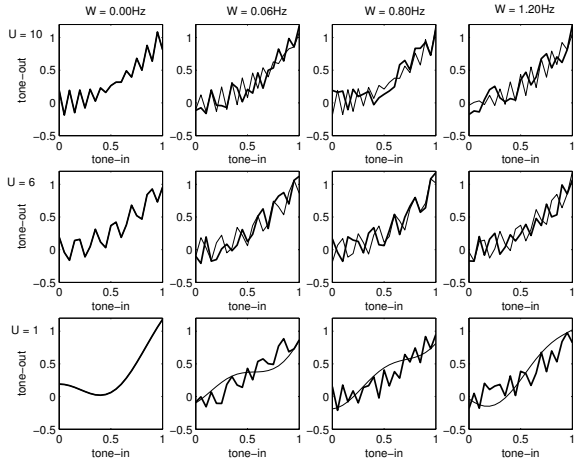

Fig. 7. Input TRC (consisting of a typical TRC with various single tonal-temporal frequency imposed on it) and its worst case steady state reconstruction, for Kalman filter designed for the bit-reversed strategy.

reconstruction is expected to improve.

V. Decomposition of the Kalman filter

We now describe our analysis of the Kalman filter (2). Since the steady state Kalman filter is M-periodic, it is difficult to talk about its frequency response. Instead, we decompose its input/output relationship using Floquet theory for periodic systems [8]. According to Floquet theory, the transition matrix $\Phi(t, t_0)$ for the $M-$ periodic discrete time (2) system can be written as:

$$\Phi(t, t_0) = P(k)\Lambda^{k-k_0}P^{-1}(k_0)$$

where $\Lambda := \Phi(M, 0)^{1/M}$ is a constant matrix and $P(k) \in \Re^{M\times M}$ is a $M-$periodic matrix sequence given by:

$$P(k) = \begin{cases} \Phi(k, 0)\Lambda^{-k} & \text{for } k \in [0, M-1] \\ P(k-M) & \text{when } k \geq M \end{cases}.$$

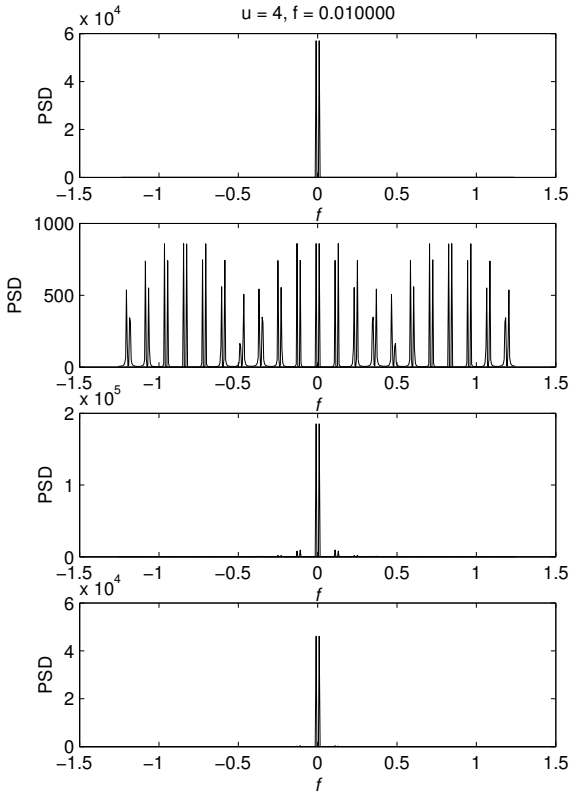

Fig. 8. Transformation of a sinusoidal temporal-spatial ($u = 4, f = 0.01$) TRC input through the three processes in the Kalman filter. From top to bottom are the temporal spectra for a particular tone: 1) original signal; 2) transformed by $GP(k+1)^{-1}B_c(k)$; after filtering by Λ; demodulation by $GP(k)G^{-1}$.

Using this decomposition and applying it to the convolution formula for (2), we have:

$$\widehat{TRC}(k) = [GP(k)G^{-1}]\cdot \left\{ G\sum_{k'=k_0}^{k-1} \Lambda^{k-k'+1}G^{-1}[GP(k'+1)^{-1}B_c(k')\cdot TRC(k')] \right\}. \quad (4)$$

Eq. (4) shows that, in the original TRC coordinates, the Kalman filter operates on the $TRC(k)$ in three steps:

1) multiplication by the periodic static operator - $y(k) \rightarrow GP(k+1)^{-1}B_c(k)\cdot y(k)$.
2) time invariant linear filtering by the filter - $y(k) \rightarrow Gx(k)$ with $x(k+1) = \Lambda x(k) + G^{-1}y(k)$
3) multiplication by another periodic static operator - $y(k) \rightarrow GP(k)G^{-1}y(k)$.

The three steps are illustrated for a low single tonal-temporal frequency TRC input signal (at one tone) in Fig. 8. Step 1 modulates the input signal by duplicating weighted copies of the original signal according to the spectrum of $GP(k'+1)^{-1}B_c(k')$. Step 2 represents a low pass filtering according to the matrix Λ which eliminates nearly all but the original signal frequency and one extra copy. Step 3 corresponds to a demodulation due to the multiplication by

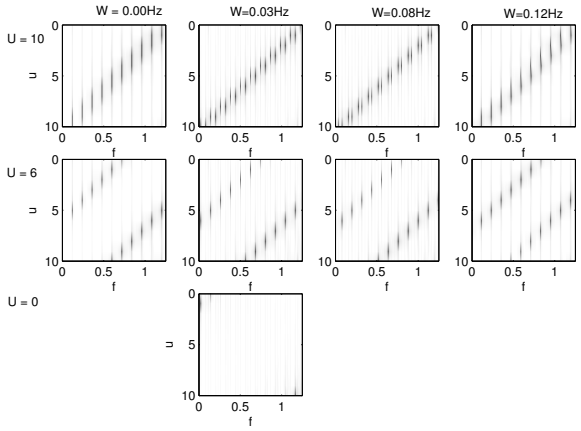

Fig. 9. Lexicographic sequence: Tonal-temporal spectral after the first transformation for various input frequencies (u, f).

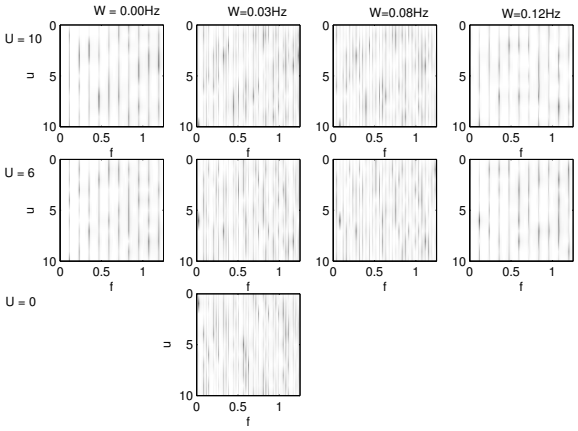

Fig. 10. Bit-reversed sequence: Tonal-temporal spectral after the first transformation for various input frequencies (u, f).

$GP(k)G^{-1}$. Interesting, the demodulation folds the high frequency copy of the signal after step 2 back to the low frequency, resulting in a reconstruction with minimal error.

The modulation effect of step 1 can also be thought of as modulating the spectral content of the map $GP(k+1)^{-1}B_c(k)$ by the input signal. Figs. 9-10 show the spectra of the signal after the first transformation for different input tonal-temporal frequencies. As the temporal frequency increases (left to right), copies of the spectral of the map approach each other on the temporal frequency domain (horizontally); and similarly as the tonal frequency increases (bottom to top), copies of the spectral of the map approach each other on the tonal frequency domain (vertical). Notice that for the lexicographical sampling sequence, the overlap is very distinct and sudden; whereas for the bit-reversed sampling sequence, the overlap process is much more diffused.

Since step 2 is a linear time invariant filter, it has a traditional frequency response as shown in Fig. 11. As expected, it has a low pass temporal response independent of the tonal frequency.

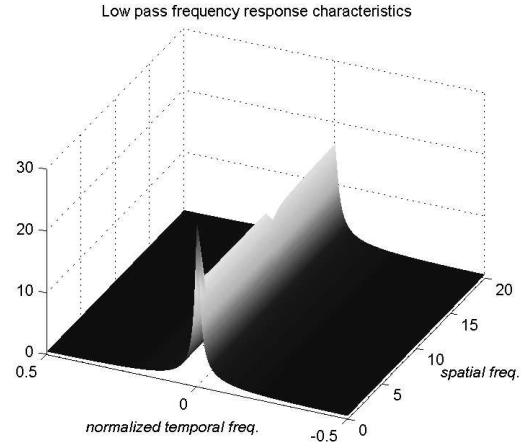

Fig. 11. The frequency response of the low-pass filter B

VI. Conclusions

Time-sequential sampling has been proposed to increase the printers' ability to sense the high dimensional time varying tone or color reproduction functions (TRC/CRC), which is useful for control of color consistency. A Kalman filter based method has been developed and shown to be effective to reconstruct the original function from the time-sequential samples. The efficacy of the time-sequential sampling scheme depends both on the signal model and the sampling strategy. Using Floquet theory, it is shown that the periodic Kalman reconstruction filter consists of a cascade of modulation, low pass filtering, and demodulation transformations. In fact, this decomposition can also be interpreted as a polyphase filter bank. This topic will be explored in the future.

References

[1] P. Y. Li and S. A. Dianat, " Robust Stabilization of Tone Reproduction Curves for Xerographic Printing Process," *IEEE Transactions on Control Systems Technology*, vol. 9, no. 2, pp. 407–415, 2001.

[2] J. P. Allebach, "Analysis of sampling-pattern dependence in time-sequential sampling of spatiotemporal signals," *Journal of Optical Society of America*, vol. 71, no. 1, pp. 99–105, January 1981.

[3] ——, "Design of antialiasing patterns for time-sequential sampling of spatiotemporal signals," *IEEE Trans. Acoustic, Speech, and Signal Processing*, vol. ASSP-32, no. 1, pp. 137–144, 1984.

[4] N. P. Willis and Y. Bresler, "Lattic-theoretic analysis of time-sequential sampling of spatiotemporal signals - part 1," *IEEE Trans. on Information Theory*, vol. 43, no. 1, pp. 190–207, January 1997.

[5] ——, "Lattic-theoretic analysis of time-sequential sampling of spatiotemporal signals - part 2: Large space-bandwidth product asymptotics," *IEEE Trans. on Information Theory*, vol. 43, no. 1, pp. 208–220, January 1997.

[6] M. A. Rahgozar and J. P. Allebach, "Motion estimation based on time-sequentially sampled imagery," *IEEE Trans. on Image Processing*, vol. 4, no. 1, pp. 48–65, January 1995.

[7] N. P. Willis and Y. Bresler, "Optimal scan for time-varying tomography i: Theoretical analysis and fundamental limitations," *IEEE Trans. on Image Processing*, vol. 4, no. 5, pp. 642–653, May 1995.

[8] F. Callier and C. A. Desoer, *Linear System Theory*. Springer Verlag, 1991.